LETTER

doi:10.1038/nature12144

Receptor binding by a ferret-transmissible H5 avian influenza virus

Xiaoli Xiong[1]*, Peter J. Coombs[1]*, Stephen R. Martin[1]*, Junfeng Liu[2], Haixia Xiao[1]†, John W. McCauley[1], Kathrin Locher[3], Philip A. Walker[1], Patrick J. Collins[1], Yoshihiro Kawaoka[4], John J. Skehel[1] & Steven J. Gamblin[1]

Cell-surface-receptor binding by influenza viruses is a key determinant of their transmissibility, both from avian and animal species to humans as well as from human to human. Highly pathogenic avian H5N1 viruses that are a threat to public health have been observed to acquire affinity for human receptors, and transmissible-mutant-selection experiments have identified a virus that is transmissible in ferrets[1–3], the generally accepted experimental model for influenza in humans. Here, our quantitative biophysical measurements of the receptor-binding properties of haemagglutinin (HA) from the transmissible mutant indicate a small increase in affinity for human receptor and a marked decrease in affinity for avian receptor. From analysis of virus and HA binding data we have derived an algorithm that predicts virus avidity from the affinity of individual HA–receptor interactions. It reveals that the transmissible-mutant virus has a 200-fold preference for binding human over avian receptors. The crystal structure of the transmissible-mutant HA in complex with receptor analogues shows that it has acquired the ability to bind human receptor in the same folded-back conformation as seen for HA from the 1918, 1957 (ref. 4), 1968 (ref. 5) and 2009 (ref. 6) pandemic viruses. This binding mode is substantially different from that by which non-transmissible wild-type H5 virus HA binds human receptor. The structure of the complex also explains how the change in preference from avian to human receptors arises from the Gln226Leu substitution, which facilitates binding to human receptor but restricts binding to avian receptor. Both features probably contribute to the acquisition of transmissibility by this mutant virus.

The importance of HA, which mediates virus binding to cell-surface sialic acid moieties in the multi-gene-dependent process of H5N1 influenza virus transmission[7], has been examined in several recent studies of ferrets infected with receptor-binding transmissible mutants[1–3]. We have studied the previously described transmissible mutant[1] that acquired the ability to transmit in respiratory droplets, without contact, from ferret to ferret. The transmissible-mutant HA contained three amino acid substitutions in or near the receptor-binding site and a fourth, about 70 Å from it, nearer to the virus membrane (Supplementary Figs 1 and 2). One of the mutations, Gln226Leu, is shared by HAs of the other droplet-transmissible H5N1 viruses recently described and was key to the acquisition of human transmissibility by the 1957 (H2) and 1968 (H3) pandemic viruses[8,9]. Such transmissibility from avian to human requires a change in binding preference from sialic acid in α2,3-linkage to galactose on carbohydrate side chains (characteristic of the virus receptors in avian enteric tracts) to sialic acid in α2,6-linkage (characteristic of human trachea airway epithelia)[10,11].

We have used two procedures to quantify the receptor-binding affinity and specificity of H5 viruses: microscale thermophoresis (MST) using recombinant HA trimers, and surface biolayer interferometry (BLI) with purified viruses. We have established a simple algorithm that enables virus binding to surfaces to be predicted from the dissociation constant ($K_{d(receptor)}$) of a single receptor interaction (Supplementary Fig. 2). Several key findings emerge. First, virus avidity for a given receptor is proportional to $K_{d(receptor)}$ to the power of the multiplicity coefficient, the factor that accounts for the contributions of multiple HA–receptor interactions that occur between a virus and a target membrane. This relationship explains how typically millimolar $K_{d(receptor)}$ values for HA affinity for its receptor can propagate to the femtomolar avidities observed for virus binding. Crucially, our data show that there is an effective upper value for the multiplicity coefficient of about 5.5, which derives from the geometry of virus particles[12] and the thermodynamics of the interactions. This limitation on virus valency explains how relatively modest decreases in $K_{d(receptor)}$, perhaps 15-fold, can lead to an almost complete loss of virus binding and accounts for the biological observations of receptor-binding specificity (Supplementary Fig. 2).

Our MST data (Fig. 1a) show that the affinity of transmissible-mutant HA for human receptor is slightly increased in comparison to HA from the wild-type A/Vietnam/1194/2004 (H5N1) (VN1194) strain (K_d = 12 mM versus 17 mM), whereas the affinity for avian receptor is greatly decreased (K_d = 32 mM versus 1.1 mM). The data also show that the transmissible-mutant HA binds about fivefold weaker to human receptor, and about tenfold weaker to avian receptor, than HA from the well-characterized 1968 pandemic H3 virus A/Aichi/2/68 (H3N2), vaccine strain X-31. The binding constants for the latter, determined here by MST, for both receptor types are in good agreement with those determined previously by NMR[13].

Our interferometry data for wild-type VN1194 H5 virus binding to human and avian receptor analogues attached to the biosensor are given in Fig. 1b, together with the data for X-31. These data show that the wild-type VN1194 H5 virus has very strong avidity towards avian receptor, as is found for nearly all avian viruses[4,8,14], and, unusually for an avian virus, almost none towards human receptor. The discrimination is such that the preference ratio (human/avian) for wild-type VN1194 H5 can only be estimated to be poorer than 5×10^{-7}. By contrast, X-31 has a preference ratio of about 10, which is similar to other pandemic viruses. To obtain information for the transmissible-mutant virus we used MST data for its HA and our empirical algorithm that relates HA affinity to virus avidity.

In Fig. 1c we present the binding curves predicted for wild-type VN1194 and transmissible-mutant viruses from the MST data using the algorithm. Importantly, there is close agreement between the experimental and predicted virus binding curves for wild-type VN1194 H5, which gives confidence in the predicted behaviour of the transmissible-mutant virus. Figure 1c shows that the transmissible-mutant virus has a preference ratio of about 200 in favour of human receptor binding, which is achieved by modest avidity for human receptor being offset by essentially undetectable binding to avian receptor. Qualitatively similar results to these have been reported previously[1]. For comparison, transmissible-mutant virus binding to human receptor is ~10^4 times

[1]MRC National Institute for Medical Research, The Ridgeway, Mill Hill, London NW7 1AA, UK. [2]Ministry of Agriculture, Key Laboratory of Plant Pathology, China Agricultural University, Yuanmingyuanxilu, 2, Beijing 100193, China. [3]Novartis Institutes for BioMedical Research, Klybeckstrasse 141, CH-4057 Basel, Switzerland. [4]Department of Pathobiological Sciences, University of Wisconsin-Madison, Madison, Wisconsin 53711, USA. †Present address: Laboratory of Protein Engineering and Vaccines, Tianjin Institute of Industrial Biotechnology, Chinese Academy of Sciences, Tianjin 300308, China.
*These authors contributed equally to this work.

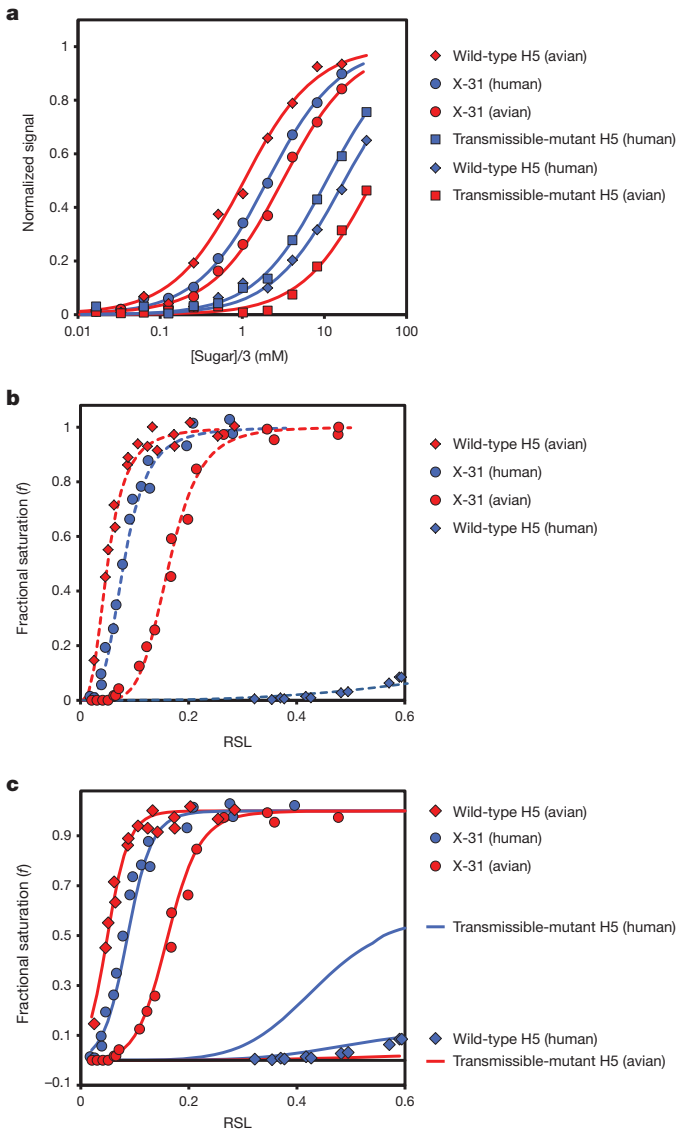

Figure 1 | HA and virus binding to human and avian receptors. a, MST data for the binding of α2,3-linked sialyl lactosamine (α2,3-SLN) and α2,6-linked sialyl lactosamine (α2,6-SLN) to HAs. Data are plotted as normalized signal change as a function of receptor sugar concentration divided by 3. For a full explanation of the normalization of the sugar concentration see Supplementary Information. **b**, BLI data for the binding of viruses to α2,3-SLN and α2,6-SLN. 30-kDa polymers containing 20% mol sugar and 5% mol biotin linked to a polyacrylamide backbone were immobilized to different levels on streptavidin-coated biosensors. Data are plotted as fractional saturation of the sensor surface as a function of relative sugar loading (RSL) for a fixed virus concentration of 100 pM. **c**, Comparison of experimental and simulated BLI data. The symbols represent the BLI data for the wild-type H5 virus. The solid lines are binding curves simulated using the HA monomer dissociation constants derived from MST experiments and the multiplicity coefficient (see Supplementary Information).

weaker than X-31, whereas its binding to avian receptor is 10^5–10^6-times weaker than X-31.

We estimate that the highest receptor loadings achieved on the BLI biosensors are of the same order as accessible sialylated glyco-conjugates on target cell surfaces (Supplementary Fig. 2). Viruses that barely bind to the biosensor at this concentration are unlikely to be able to bind effectively to cells. It seems clear, therefore, that although the transmissible-mutant virus binds human receptor more weakly than pandemic viruses, about half of the virus will be bound at the receptor densities found on cell surfaces, a conclusion consistent with its observed transmissibility. On the other hand the transmissible-mutant virus would not bind effectively to cells with predominantly avian receptors. As a consequence the specificity properties of the transmissible-mutant virus would favour infection of cells in the human upper respiratory tract that have been shown to display α2,6-linked sialic acids. At the same time, the loss of avian receptor binding would also prevent the sequestration of the virus by airway mucins, which are rich sources of α2,3-linked sialic acid[15]. Avoidance of mucins is probably important for the ferret transmissibility of the transmissible-mutant virus given that its human-receptor-binding properties are modest compared to pandemic viruses.

To understand the molecular basis of the altered affinity and specificity of the transmissible-mutant HA we determined its crystal structure, and that of wild-type VN1194 (clade 1) and A/turkey/Turkey/1/2005 (H5N1) (tyTy) (clade 2) H5 HAs in complex with human receptor analogues (Fig. 2, Supplementary Table 1 and Supplementary Fig. 1). The most notable feature of these structures is the different orientation of galactose at position 2 (Gal-2) and *N*-acetylglucosamine at position 3 (GlcNAc-3) of the receptor in the transmissible-mutant HA complex compared with their arrangement in both wild-type HA complexes (Fig. 2). In the transmissible-mutant complex, Gal-2 adopts a *cis* configuration about the glycosidic bond with sialic acid, and GlcNAc-3 exits the receptor-binding site towards the 190-helix (residues 187–197) (Fig. 2a, b) This orientation of Gal-2 and GlcNAc-3 is very similar to that in complexes formed between human receptor and HAs from the 1918 (H1), 1957 (H2) and 1968 (H3) pandemic viruses[4,5] (Fig. 3a). However, it is in marked contrast to that seen in the wild-type H5 HA structures (Fig. 2e, g). Although only the first two sugars are ordered in the VN1194 complex, compared with three in the tyTy complex, sialic acid at position 1 of the receptor (Sia-1) and Gal-2 adopt the same conformation in both. In these cases (and all other mutant H5 HAs we have examined (X.X. *et. al*, unpublished observations)), Gal-2 also adopts a *cis* configuration about the glycosidic bond with sialic acid but it is rotated by approximately 90° about its C6–C5 bond such that GlcNAc-3 exits from the side of the receptor-binding site, over the 130-loop (residues 132–138). This mode of human-receptor binding has not been reported for any other avian or human HA. It seems to be enabled by the formation of a hydrogen bond between the 3′ hydroxyl of Gal-2 with the main-chain carbonyl at residue 225 (Fig. 3b). This interaction is facilitated by the low position in the site adopted by Gln 226, which is stabilized by a hydrogen bond between its side chain and the hydroxyl of Ser 137.

The most obvious explanation for the difference in Gal-2 orientation in the complex formed by the transmissible-mutant HA with the human receptor is the presence at the base of the receptor-binding site of the hydrophobic leucine residue at position 226, in place of the polar glutamine residue found in wild-type H5 HAs. The structural effect of this Gln226Leu mutation in the transmissible mutant appears similar to that caused by the same substitution associated with the conversion of avian H2 and H3 to human viruses. In all three cases the introduction of the hydrophobic residue increases the separation between the 220- and 130-loops by about 1 Å, and residues 224 and 225 on the 220-loop (residues 220–228) sit about 1.4 Å higher in the site as a consequence of human-receptor binding (Supplementary Fig. 1).

To understand the loss of avian-receptor binding by transmissible-mutant HA we determined its structure, and that of the wild-type H5 HAs, in complex with an avian receptor analogue (Fig. 2c, f, h and Supplementary Fig. 1k–o). The most notable feature of these complexes is that, whereas both wild-type HAs bind avian receptor in the typical fashion of all avian HAs reported to date[4,16,17] (Fig. 2f, h), the transmissible-mutant HA binds in a substantially different way with Gal-2 adopting a *cis*, rather than a *trans*, conformation about the glycosidic bond with sialic acid (Fig. 2c). As a result, Gal-2 appears face-on in the transmissible-mutant complex in Fig. 2 whereas it is edge-on in the wild-type H5 HA complexes. The altered orientation of Gal-2 and of GlcNAc-3 also results in a quite different trajectory for the avian receptor in the transmissible-mutant HA complex compared

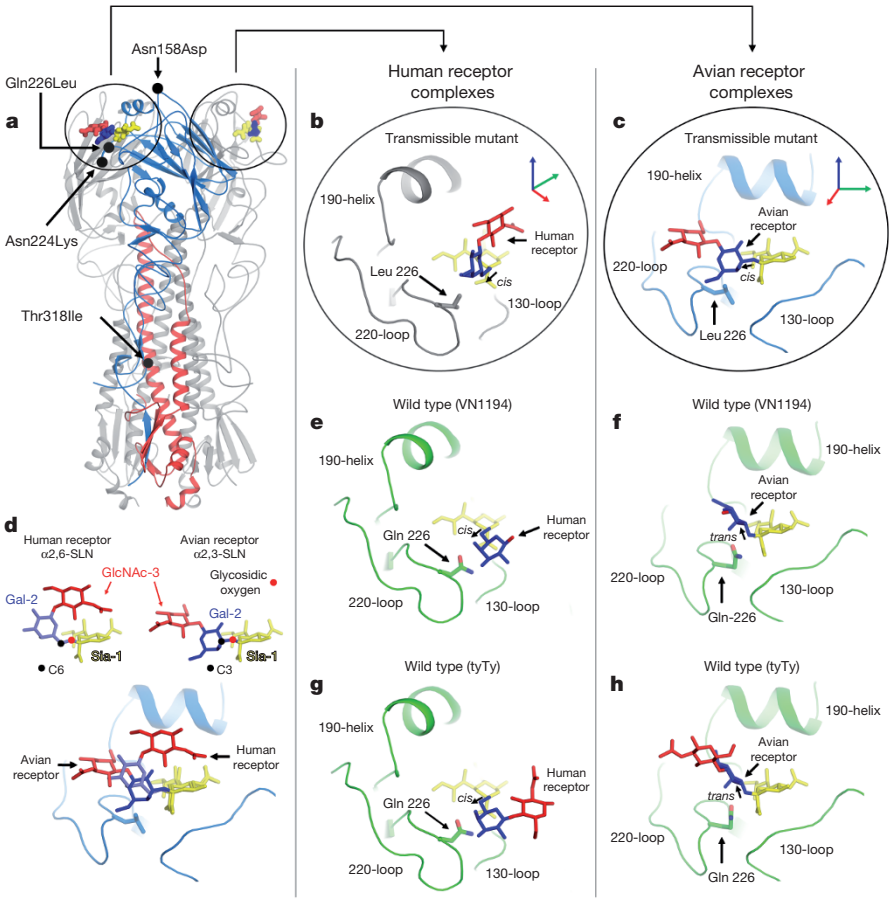

Figure 2 | Crystal structures of receptor complexes of wild-type H5 and transmissible-mutant HAs. **a**, Ribbons representation of an HA trimer of transmissible mutant with one monomer coloured in blue (HA-1) and red (HA-2), and the other two monomers shown in grey. For two of the monomers the structures of the bound receptor analogues are encircled and magnified in **b** (human receptor) and **c** (avian receptor). The locations of the four mutations associated with the transmissible mutant are indicated by solid black dots and are labelled. **b**, The receptor-binding site of the transmissible-mutant HA containing human receptor with the three sugars coloured in red (GlcNAc-3), blue (Gal-2) and yellow (Sia-1). The structural elements that form the edges of the receptor binding site are labelled: 130-loop, 190-helix and 220-loop. **c**, The receptor-binding site of a second monomer (rotated about the vertical axis) showing bound avian receptor. **d**, The components of the human (left) and avian (right) receptor and their distinctive linkage types in the upper part and an overlap of the same two ligands shown in orientation of **c** in the lower part. **e**–**h**, The receptor-binding sites of wild-type VN1194 and tyTy H5 HA with bound human receptor (**e** and **g**, respectively) viewed in the same orientation of the complex as **b**, and wild-type VN1194 and tyTy H5 HA bound to avian receptor (**f** and **h**, respectively) in the same orientation of the complex as **c**.

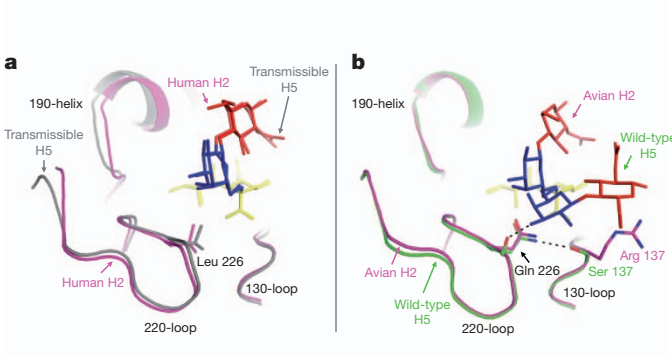

Figure 3 | Comparison of H5 and H2 HA complexes with human receptor. **a**, The receptor-binding site of transmissible-mutant HA (grey) overlapped with human H2 HA (purple) viewed in the same orientation as Fig. 2b showing the close similarity in the conformation of the human receptor in the two complexes. **b**, A similar view of the overlap of the receptor-binding complexes shows that the human receptor adopts a substantially different conformation in the wild-type H5 HA (green) than in the avian H2 HA (purple) complex.

with the wild-type H5 HA complexes. This mode of binding avian receptor by transmissible-mutant HA is shared by both H2 and H3 pandemic virus HAs[4,5] (Supplementary Fig. 1).

In addition to the Gln226Leu mutation, transmissible-mutant HA contains three other amino acid substitutions: Asn158Asp, Asn224Lys and Thr318Ile (Fig. 2a and Supplementary Fig. 1). Asn158Asp results in the loss of a site for glycosylation in clade 1 H5 HAs (many clade 2 H5 HAs also lack this glycosylation sequon). Simple modelling studies based on our structure of the complexes formed between wild-type and the transmissible-mutant HA with human receptor suggest that the presence of a large carbohydrate side chain at residue 158 might sterically block receptor binding to cell-surface sialic acids[18] (Supplementary Fig. 1a). Mutation of the glycosylation site would remove this potential impediment and thus facilitate the observed transmissibility in ferrets[1,2].

Residue 224 is located on the rim of the receptor-binding site (Fig. 2a, b and Supplementary Fig. 1) with its side chain oriented away from the site. It is not apparent that it influences receptor binding directly. However, the substitution of a lysine residue at this position introduces a basic residue that may, like similar mutations that have been described in H5 viruses isolated from humans[19], enhance virus binding to cell surfaces through non-specific electrostatic interactions. It is notable in this regard that in two of the respiratory-droplet-transmissible-mutant H5 viruses that have been described, in addition

to the Gln226Leu amino acid substitution, there have been mutations that introduce basic amino acids: Gln196Arg[3] and Asn224Lys[1]. These observations suggest that increases in positive charge at the membrane-distal surface of HA may be favourable for non-specific interaction with negatively charged cell-surface components[20,21]. Given the relatively modest specific binding that the transmissible-mutant HA displays towards human receptors, such a non-specific contribution may favour transmissibility.

Residue 318 is 70 Å away from the receptor-binding site (Fig. 2a and Supplementary Fig. 1) and is unlikely to influence receptor binding directly. However, it has been shown to increase the thermal stability of the transmissible-mutant HA[1], which is consistent with the known effects of mutations in similar locations in the intra-and inter-subunit interfaces of HA[22]. Our structure shows how the Thr318Ile mutation results in the isoleucine residue packing against the hydrophobic surface formed by Trp 21 in the 'fusion peptide' and Val 48 and Val 52 in the middle of helix A of the same subunit (Supplementary Fig. 1c) This interaction would stabilize the positions of both the fusion peptide and helix A, and as a consequence counteract the destabilizing effects of the three mutations in the membrane-distal locations[23], resulting in retention of the wild-type HA fusion pH[1].

As the first step in virus infection, HA receptor binding of appropriate affinity and specificity is an obvious requirement for the spread of infection between individuals and between species. For pandemic influenza viruses that originate in avian species the acquisition of both properties is required. Avian influenza viruses of the H5 subtype remain a threat because they have been shown to have the ability to infect humans and because the infections that they have caused in humans and in other species are extremely severe. Genetically, HAs of the H5 subtype are most closely related to HAs of the H1 and H2 subtypes, both of which have been the source of pandemic influenza virus HAs. However, the mechanism by which avian H1 viruses acquired the ability to infect and spread in humans is distinct from that used by avian H2 viruses. The H1 virus HA required the Glu190Asp and Gly225Asp mutations[9,24,25] in the receptor-binding site. By contrast, the H2 HA required the Gln226Leu and Gly228Ser mutations[9,14,26,27]. Importantly, in relation to observations on the transmissible-mutant virus, H2 precursor viruses, containing only the Gln226Leu mutation, were isolated in 1957 (ref. 9) and a similar H2 virus with the same single mutation has recently been shown to acquire transmissibility in ferrets[28]. The structural consequences of the Gln226Leu substitution, widening of the gap between the 130- and 220-loops at the edges of the receptor-binding site, and generation of a hydrophobic environment at the base of the site, are very similar for the transmissible-mutant HA and for the HA of the H2 pandemic virus and are broadly similar to what occurs in the more distantly related HA of the H3 pandemic virus[17] (Supplementary Fig. 1).

In some respects the properties of the transmissible mutant described here suggest that H5 viruses could take a similar evolutionary pathway in humans to that followed in 1957 and 1968 by avian H2 and H3 viruses. Thus, the preference of the transmissible mutant for binding to human versus avian receptors, and the structural manner by which it binds them, are highly characteristic of pandemic viruses. On the other hand, the transmissible mutant achieves its 200-fold preference for human receptor by essentially losing its binding potential for avian receptor. This property distinguishes it from known pandemic viruses. Whether or not these properties are shared by the other two transmissible H5 mutants[2,3] remains to be determined.

The loss of affinity for avian receptor noted here also implies that the species in which a transmissible mutant of this sort may evolve would be restricted to either birds (such as quail[29]) or mammals (such as pigs or humans[30]) which could provide an abundance of human receptors. This restriction may also distinguish the transmissible mutant from viruses that were precursors of the H2 and H3 pandemics. Both avian H2 and H3 viruses with high avidity for both avian and human receptors have been identified[4], and they may have been directly transferred to humans from waterfowl, the main source of avian influenza viruses.

METHODS SUMMARY

Influenza viruses were grown in hens' eggs and purified by sucrose density gradient centrifugation, according to standard protocols. HA trimers were purified after proteolytic release from these viruses. HAs for wild-type A/Vietnam/1194/2004 (H5N1) (VN1194) and A/turkey/Turkey/1/2005 (H5N1) (tyTy) and the transmissible-mutant H5 were sub-cloned into a modified pAcGP67A vector that carries a tobacco etch virus (TEV) protease site, a trimerization foldon and a His tag. Protein was expressed in Sf9 cells and purified as described previously[21]. MST measurements were performed using a NanoTemper Monolith NT.115 instrument (NanoTemper Technologies GmbH). BHA samples (HA released from virus by bromelain digestion) were labelled with the amine-reactive dye NT-647 using the Monolith NT.115 Protein Labelling Kit RED-NHS. Binding curves were generated from the sodium salts of α2,3-SLN and α2,6-SLN (obtained from Dextra). For BLI, virus binding to defined receptor analogues was measured on an Octet RED biolayer interferometer (ForteBio). Biotinylated α2,3-SLN and α2,6-SLN were purchased from Lectinity Holdings Inc. Binding of viruses (at 100 pM) was measured at 25 °C in a 30–50-min association step. All solutions also contained 10 μM oseltamivir carboxylate (Roche) and 10 μM zanamivir (GSK) to prevent cleavage of the receptor analogues by the viral neuraminidase. The (relative) amount of virus bound to the biosensor at different RSLs was calculated from the amplitude of the response at the end of the association step. HA was crystallized according to standard procedures and HA–receptor complexes were prepared by soaking HA crystals in crystallization solution supplemented with 40 mM receptor analogues 2,3-SLN or 2,6-SLN. Diffraction data were collected at 100 K at the Diamond Synchrotron, processed with Mosflm or XDS and subsequent calculations carried out using the CCP4 suite. Structures were built with Coot and refined with Refmac.

Full Methods and any associated references are available in the online version of the paper.

Received 7 December 2012; accepted 5 April 2013.
Published online 24 April 2013.

1. Imai, M. *et al.* Experimental adaptation of an influenza H5 HA confers respiratory droplet transmission to a reassortant H5 HA/H1N1 virus in ferrets. *Nature* **486,** 420–428 (2012).
2. Herfst, S. *et al.* Airborne transmission of influenza A/H5N1 virus between ferrets. *Science* **336,** 1534–1541 (2012).
3. Chen, L. M. *et al. In vitro* evolution of H5N1 avian influenza virus toward human-type receptor specificity. *Virology* **422,** 105–113 (2012).
4. Liu, J. *et al.* Structures of receptor complexes formed by hemagglutinins from the Asian Influenza pandemic of 1957. *Proc. Natl Acad. Sci. USA* **106,** 17175–17180 (2009).
5. Eisen, M. B., Sabesan, S., Skehel, J. J. & Wiley, D. C. Binding of the influenza A virus to cell-surface receptors: structures of five hemagglutinin–sialyloligosaccharide complexes determined by X-ray crystallography. *Virology* **232,** 19–31 (1997).
6. Xu, R., McBride, R., Nycholat, C. M., Paulson, J. C. & Wilson, I. A. Structural characterization of the hemagglutinin receptor specificity from the 2009 H1N1 influenza pandemic. *J. Virol.* **86,** 982–990 (2012).
7. Hatta, M. *et al.* Growth of H5N1 influenza A viruses in the upper respiratory tracts of mice. *PLoS Pathog.* **3,** e133 (2007).
8. Connor, R. J., Kawaoka, Y., Webster, R. G. & Paulson, J. C. Receptor specificity in human, avian, and equine H2 and H3 influenza virus isolates. *Virology* **205,** 17–23 (1994).
9. Matrosovich, M. *et al.* Early alterations of the receptor-binding properties of H1, H2, and H3 avian influenza virus hemagglutinins after their introduction into mammals. *J. Virol.* **74,** 8502–8512 (2000).
10. Couceiro, J. N., Paulson, J. C. & Baum, L. G. Influenza virus strains selectively recognize sialyloligosaccharides on human respiratory epithelium; the role of the host cell in selection of hemagglutinin receptor specificity. *Virus Res.* **29,** 155–165 (1993).
11. Shinya, K. *et al.* Avian flu: influenza virus receptors in the human airway. *Nature* **440,** 435–436 (2006).
12. Calder, L. J., Wasilewski, S., Berriman, J. A. & Rosenthal, P. B. Structural organization of a filamentous influenza A virus. *Proc. Natl Acad. Sci. USA* **107,** 10685–10690 (2010).
13. Sauter, N. K. *et al.* Hemagglutinins from two influenza virus variants bind to sialic acid derivatives with millimolar dissociation constants: a 500-MHz proton nuclear magnetic resonance study. *Biochemistry* **28,** 8388–8396 (1989).
14. Gambaryan, A. S. *et al.* Specification of receptor-binding phenotypes of influenza virus isolates from different hosts using synthetic sialylglycopolymers: non-egg-adapted human H1 and H3 influenza A and influenza B viruses share a common high binding affinity for 6′-sialyl(*N*-acetyllactosamine). *Virology* **232,** 345–350 (1997).
15. Matrosovich, M. & Klenk, H. D. Natural and synthetic sialic acid-containing inhibitors of influenza virus receptor binding. *Rev. Med. Virol.* **13,** 85–97 (2003).

16. Ha, Y., Stevens, D. J., Skehel, J. J. & Wiley, D. C. X-ray structures of H5 avian and H9 swine influenza virus hemagglutinins bound to avian and human receptor analogs. *Proc. Natl Acad. Sci. USA* **98,** 11181–11186 (2001).
17. Ha, Y., Stevens, D. J., Skehel, J. J. & Wiley, D. C. X-ray structure of the hemagglutinin of a potential H3 avian progenitor of the 1968 Hong Kong pandemic influenza virus. *Virology* **309,** 209–218 (2003).
18. Wang, W. *et al.* Glycosylation at 158N of the hemagglutinin protein and receptor binding specificity synergistically affect the antigenicity and immunogenicity of a live attenuated H5N1 A/Vietnam/1203/2004 vaccine virus in ferrets. *J. Virol.* **84,** 6570–6577 (2010).
19. Yamada, S. *et al.* Haemagglutinin mutations responsible for the binding of H5N1 influenza A viruses to human-type receptors. *Nature* **444,** 378–382 (2006).
20. Arinaminpathy, N. & Grenfell, B. Dynamics of glycoprotein charge in the evolutionary history of human influenza. *PLoS ONE* **5,** e15674 (2010).
21. Lin, Y. P. *et al.* Evolution of the receptor binding properties of the influenza A(H3N2) haemagglutinin. *Proc. Natl Acad. Sci. USA Nature* **109,** 21474–21479 (2012).
22. Ruigrok, R. W. *et al.* Conformational changes in the hemagglutinin of influenza virus which accompany heat-induced fusion of virus with liposomes. *Virology* **155,** 484–497 (1986).
23. Steinhauer, D. A. *et al.* Studies using double mutants of the conformational transitions in influenza hemagglutinin required for its membrane fusion activity. *Proc. Natl Acad. Sci. USA* **93,** 12873–12878 (1996).
24. Gamblin, S. J. *et al.* The structure and receptor binding properties of the 1918 influenza hemagglutinin. *Science* **303,** 1838–1842 (2004).
25. Stevens, J. *et al.* Glycan microarray analysis of the hemagglutinins from modern and pandemic influenza viruses reveals different receptor specificities. *J. Mol. Biol.* **355,** 1143–1155 (2006).
26. Rogers, G. N. *et al.* Host-mediated selection of influenza virus receptor variants. Sialic acid-α2,6Gal-specific clones of A/duck/Ukraine/1/63 revert to sialic acid-α2,3Gal-specific wild type *in ovo*. *J. Biol. Chem.* **260,** 7362–7367 (1985).
27. Rogers, G. N. *et al.* Single amino acid substitutions in influenza haemagglutinin change receptor binding specificity. *Nature* **304,** 76–78 (1983).
28. Pappas, C. *et al.* Receptor specificity and transmission of H2N2 subtype viruses isolated from the pandemic of 1957. *PLoS ONE* **5,** e11158 (2010).
29. Gambaryan, A. S. *et al.* Receptor-binding profiles of H7 subtype influenza viruses in different host species. *J. Virol.* **86,** 4370–4379 (2012).
30. Baigent, S. J. & McCauley, J. W. Influenza type A in humans, mammals and birds: determinants of virus virulence, host-range and interspecies transmission. *BioEssays* **25,** 657–671 (2003).

Supplementary Information is available in the online version of the paper.

Acknowledgements We are grateful to staff at the Diamond Light Source Synchrotron for assistance and beamline access under proposal 7707, E. Christodoulou and S. Vachieri for discussions on protein expression, the staff of the NIMR Large Scale Laboratory, L Haire for assistance with crystallization experiments and S. Smerdon and P. Rosenthal for discussions. H.X. was supported by BBSRC (award number BB/E010806). This work was funded by the Medical Research Council through programmes U117584222, U117512723 and U117570592.

Author Contributions X.X., P.J.C., S.R.M., J.L., H.X., J.W.M., K.L., P.A.W., P.C., Y.K., J.J.S. and S.J.G. all performed experiments and contributed to the writing of the manuscript.

Author Information Structural data have been deposited with the Protein Data Bank under accession codes 4BGW, 4BGX, 4BGY, 4BGZ, 4BH0, 4BH1, 4BH2, 4BH3 and 4BH4. Reprints and permissions information is available at www.nature.com/reprints. The authors declare no competing financial interests. Readers are welcome to comment on the online version of the paper. Correspondence and requests for materials should be addressed to S.J.G. (sgambli@nimr.mrc.ac.uk) or J.J.S. (skeheljj@nimr.mrc.ac.uk).

METHODS

MST. MST measurements were performed using a NanoTemper Monolith NT.115 instrument (NanoTemper Technologies GmbH). HA samples were labelled with the amine-reactive dye NT-647 using the Monolith NT.115 Protein Labelling Kit RED-NHS. Labelling levels (generally in the range 0.3–0.4 dye molecules per HA monomer) were determined using $\varepsilon_{280} = 74090$ (H3) and 83030 (H5) $M^{-1}cm^{-1}$ for the HA monomer concentration, and $\varepsilon_{647} = 250{,}000$ $M^{-1}cm^{-1}$ for the dye concentration. Sodium salts of α2,3-SLN and α2,6-SLN (obtained from Dextra) were dissolved to a final concentration of 50–100 mM in PBS buffer containing 0.05% Tween-20 and labelled HA at a concentration of ~50 nM. This stock solution was then serially diluted 1:1 using the same buffer to give 12 working solutions with different sugar concentrations but the same fluorophore concentration. These solutions were then loaded into standard treated capillaries and MST measurements were made at 25 °C using 20% light-emitting diode power and 40% infrared-laser power. The laser-on time was 30 s and laser-off time 5 s. All measurements were made at least five times.

BLI. Virus binding to defined receptor analogues was measured on an Octet RED biolayer interferometer (ForteBio). Biotinylated α2,3-SLN and α2,6-SLN were purchased from Lectinity Holding. These were approximately 30-kDa polymers containing 20% mol sugar and 5% mol biotin linked to a polyacrylamide backbone. The polymers were immobilized on streptavidin biosensors (ForteBio) at concentrations ranging from 0.01–1.5 $\mu g\,ml^{-1}$. The RSL of the biosensor was calculated from the amplitude of the response at the end of the 5–10-min loading step. The maximum response at complete saturation was ~0.6 nm. Binding of viruses (at 100 pM) was measured at 25 °C in a 30–50-min association step. The buffer was 10 mM HEPES, pH 7.4, 150 mM NaCl, 3 mM EDTA and 0.005% Tween-20. All solutions also contained 10 μM oseltamivir carboxylate (Roche) and 10 μM zanamivir (GSK) to prevent cleavage of the receptor analogues by the viral neuraminidase. The (relative) amount of virus bound to the biosensor at different RSLs was calculated from the amplitude of the response at the end of the association step. These measured amplitudes were normalized by dividing by the maximum response (typically 5–6 nm) and this normalized response was plotted as a function of the RSL (see Fig. 1a and Supplementary Fig. 2). These normalized virus binding response curves report the fractional saturation of the sensor surface (f) and smooth lines through the curves were generated by fitting the data to a simple variant of the Hill equation:

$$f = \frac{[\mathrm{RSL}]^n}{[\mathrm{RSL}_{0.5}]^n + [\mathrm{RSL}]^n}$$

In which RSL is the relative sugar loading, $\mathrm{RSL}_{0.5}$ is the relative sugar loading at half saturation ($f = 0.5$), and n is a Hill coefficient.

Crystallography. The HA of VN1194 was purified from vaccine strain virus RG14 grown in embryonated chicken eggs. HAs of tyTy and the transmissible mutant were expressed in Sf9 insect cells. Following previously published methods[22] all H5 HAs were purified as trypsin released ectodomains in the final buffer (10 mM Tris-HCl, pH 8.0, 50 mM NaCl). VN1194 HA was crystallized from 0.1 M HEPES, pH 7.0, 0.05 M $MgCl_2$, 28–30% PEG 550. tyTy HA was initially crystallized from Bis-tris propane, pH 7.5, 0.2 M K/$NaPO_4$, pH 7.0, 20% PEG 3350 and crystals were improved by seeding in Bis-tris propane, pH 7.5, 0.05–0.15 M K/NaPO4, pH 7.0, 15–18% PEG 3350. The transmissible mutant was crystallized from 0.1 M HEPES, pH 7.0, 25–30% Jaffamine ED-2001. Ligand-soaking experiments were performed by soaking the crystals in crystallization solution supplemented with 40 mM receptor analogues for 16 h. VN1194 and transmissible-mutant crystals were frozen in liquid nitrogen directly from the drop. tyTy HA crystals were cryo-protected by addition of 25% ethylene glycol before freezing.

Diffraction data were collected on Diamond beamlines at 100 K, and processed in the XIA2 pipeline, before being scaled by Scala from the CCP4 suite. Structures were determined by molecular replacement in Phaser using the VN1194 structure as a search model (PDB code, 2IBX). MolProbity was used to validate the final structures.